CONDENSED MATTER PHYSICS

Slow dynamics of electrons at a metal–Mott insulator boundary in an organic system with disorder

Tetsuaki Itou,[1,2]* Eri Watanabe,[3] Satoru Maegawa,[3] Akiko Tajima,[4] Naoya Tajima,[4,5] Kazuya Kubo,[4,6]† Reizo Kato,[4] Kazushi Kanoda[7]

The Mott transition—a metal-insulator transition caused by repulsive Coulomb interactions between electrons—is a central issue in condensed matter physics because it is the mother earth of various attractive phenomena. Outstanding examples are high–T_c (critical temperature) cuprates and manganites exhibiting colossal magneto-resistance. Furthermore, spin liquid states, which are quantum-fluctuation–driven disordered ground states in antiferromagnets, have recently been found in magnetic systems very near the Mott transition. To date, intensive studies on the Mott transition have been conducted and appear to have established a nearly complete framework for understanding the Mott transition. We found an unknown type of Mott transition in an organic spin liquid material with a slightly disordered lattice. Around the Mott transition region of this material under pressure, nuclear magnetic resonance experiments capture the emergence of slow electronic fluctuations of the order of kilohertz or lower, which is not expected in the conventional Mott transition that appears as a clear first-order transition at low temperatures. We suggest that they are due to the unconventional metal-insulator fluctuations emerging around the disordered Mott transition in analogy to the slowly fluctuating spin phase, or Griffiths phase, realized in Ising spin systems with disordered lattices.

INTRODUCTION

The Mott transition is realized when the U/W ratio of the electron correlation energy U to the typical kinetic energy (or bandwidth) W exceeds a critical value. In several real materials, pressure can experimentally control W, causing pressure-induced Mott transitions. Extensive research on the Mott transition has been conducted over the last few decades and has established a consensus that the Mott transition is of the first order at low temperatures and a crossover at high temperatures in the pressure-temperature phase diagram (1–6), although the nature of the criticality is under debate; unconventional critical exponents are indicated by conductivity (7) and nuclear magnetic resonance (NMR) relaxation rate (8) and by the theories of marginal quantum criticality (9) and dynamical mean-field theory (DMFT) (10), whereas the mean-field or Ising values are indicated by expansivity (11) and conductivity (12, 13) as well as theoretical studies (14–16).

The experimental studies on the Mott transition have been conducted in both organic and inorganic materials. One studied type of organic Mott insulator is the $X[Pd(dmit)_2]_2$ family, where dmit denotes an organic ligand, 1,3-dithiole-2-thione-4,5-dithiolate, and X is a monovalent closed-shell cation (17). In particular, $X[Pd(dmit)_2]_2$ salts with X = $EtMe_3Sb$ and $EtMe_3P$ have attracted considerable attention from the magnetism perspective because they have quasi–two-dimensional (2D) nearly regular triangular lattices. The $EtMe_3P$ salt shows a valence bond–solid ground state with a spin gap (18), whereas

the $EtMe_3Sb$ salt shows a spin liquid ground state (19), the nature of which remains highly controversial (20–24). The important difference between the crystal structures of these two salts is that the $EtMe_3Sb$ salt (space group C2/c) has a quenched random orientation of the ethyl groups in the cation layer (17), as shown in Fig. 1A, whereas the $EtMe_3P$ salt (space group $P2_1/m$) has an ordered orientation of the ethyl groups with no randomness.

The $EtMe_3P$ salt undergoes a conventional Mott transition under pressure, as expected; transport studies have revealed that the $EtMe_3P$ salt shows a first-order Mott transition with a critical end point of 30 K (13, 25). However, the $EtMe_3Sb$ salt, which has inevitable randomness in the cation layer, does not show any resistivity jump indicating a first-order transition, as shown in Fig. 1B. Note that, even in the highly conductive state stabilized under high pressure, the resistivity increases slightly during cooling at low temperatures. This behavior is likely the manifestation of the randomness, and the randomness could be responsible for the peculiarity in the Mott transition in the $EtMe_3Sb$ salt. Stimulated by this observation, we further examined the nature of the Mott transition in the $EtMe_3Sb$ salt by ^{13}C NMR and found anomalously slow dynamics of electrons never seen before.

RESULTS

Figure 2 shows the temperature dependence of the spin-lattice relaxation rate (T_1^{-1}; see Materials and Methods) of the $EtMe_3Sb$ salt, which reflects the magnitude of the fluctuations of the internal magnetic field on the ^{13}C nuclei on a megahertz time scale. In the Mott-insulating state at ambient pressure, T_1^{-1} shows a large drop below 1 K. This drop appears to suggest a marginal spin-gapped ground state, as discussed by the works of Itou and co-workers (21, 23), whereas there are also reports claiming the existence of fully gapless fermion-like excitations (20, 22, 24). For pressures below 5 kbar, the temperature dependence of T_1^{-1} is almost the same, indicating that the nature of the Mott-insulating phase is maintained in this pressure region. However, at higher pressures, T_1^{-1} is depressed and comes to follow the Korringa relation, namely, T_1^{-1} decreases in proportion to the temperature. This

behavior indicates that the Mott boundary is situated at approximately 6 kbar, consistent with the resistivity result shown in Fig. 1B.

Figure 3A shows the temperature dependence of the spin-spin relaxation rate (T_2^{-1}; see Materials and Methods) of $X[Pd(dmit)_2]_2$. The spin-spin relaxation rate T_2^{-1} is generally expressed as the sum of two different components—the Lorentzian relaxation rate T_{2l}^{-1} and the Gaussian relaxation rate T_{2g}^{-1} ($T_2^{-1} = T_{2l}^{-1} + T_{2g}^{-1}$)—which measure the electron fluctuations on a kilohertz time scale and nuclear-nuclear magnetic coupling, respectively. In $X[Pd(dmit)_2]_2$ systems, T_{2g}^{-1} is determined by the nuclear dipolar interaction and is, thus, invariant with respect to temperature. A constant value of 640 s^{-1} is observed in the EtMe$_3$P salt, the conventional Mott insulator. In contrast, the EtMe$_3$Sb salt shows appreciable enhancement relative to this value. This enhancement indicates the significant contribution of T_{2l}^{-1}, which can be estimated by subtracting T_{2g}^{-1} (=640 s^{-1}) from the observed value of T_2^{-1}, and is shown on the right axis of Fig. 3A (for details, see the Supplementary Materials). Note that, although the cation has the rotational motion of the methyl groups (23), this lattice motion does not contribute to the relaxations (for details, see the Supplementary Materials).

In typical electron systems, no significant difference in the intensity of the fluctuations between the kilohertz and megahertz regions should exist, namely, $T_{2l}^{-1} = T_1^{-1}$,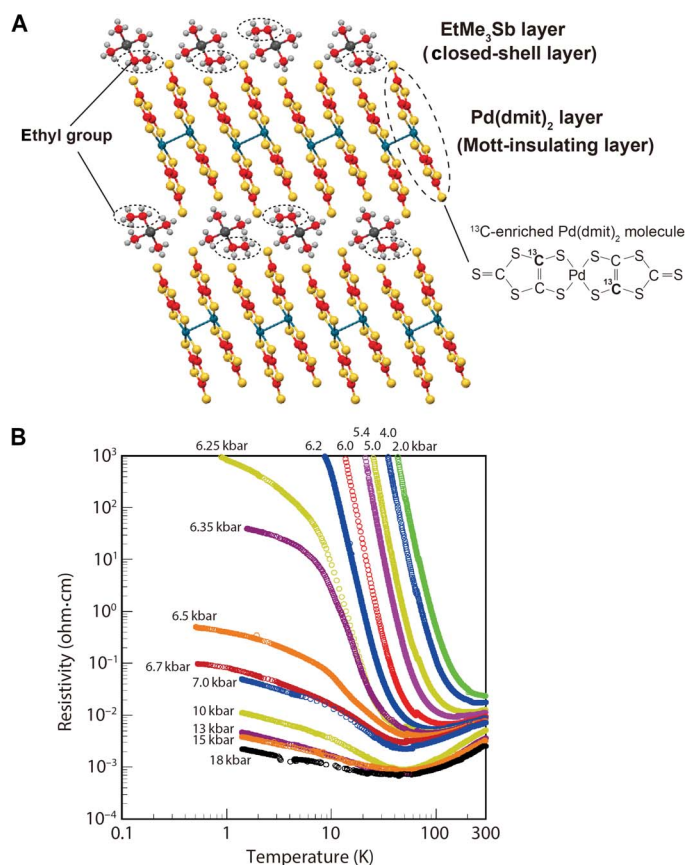 because the electron fluctuations are dominated by the Hamiltonian of the system and, thus, generally white well below the energy scales of the transfer integrals, exchange interactions, and Coulomb repulsions, all of which reside in the terahertz region. In contrast to this common understanding, in the EtMe$_3$Sb salt, T_{2l}^{-1} increases to ~10^3 s^{-1} at low temperatures, which is several orders of magnitude greater than T_1^{-1}, as seen in Figs. 2 and 3A. This difference signifies the emergence of an unusual electronic phase that has extraordinarily slow fluctuations, where the kilohertz fluctuations are several orders of magnitude stronger than the megahertz ones.

The anomalous electronic fluctuations should occur in either the spin or the charge channel: (i) direct spin fluctuations, which cause NMR relaxations through hyperfine interactions, and (ii) charge fluctuations, which also cause NMR relaxations through appendant temporal modulations of hyperfine interactions accompanying the charge fluctuations. Note that the temperature dependence of the enhancement of T_{2l}^{-1} is not monotonous [this can be distinctly observed around the Mott boundary pressure (7 kbar)], as shown in Fig. 3A. At ambient pressure, T_{2l}^{-1} increases appreciably below 30 K, peaks at approximately 12 K, and then monotonously decreases down to 1 K. At 4 kbar, the peak is somewhat suppressed; however, a separate increase in T_{2l}^{-1} appears below 2.5 K. When the pressure is increased to 7 kbar, the low-temperature increase in T_{2l}^{-1} is substantially enhanced, whereas the high-temperature peak is not. At 15 kbar, both of the features are suppressed. Two structures are thus evident in the temperature profile of T_{2l}^{-1}, as shown in Fig. 3B, implying two different types of slow fluctuations. One type is a component that grows at low temperatures, whereas the other is a component that shows a peak at 10 to 30 K. The former component (the red component in Fig. 3B) is markedly prominent at 7 kbar, which is near the Mott boundary. Therefore, the former component is most likely attributable to charge fluctuations related to the Mott transition, that is, slow fluctuations between the metallic state and the Mott-insulating state develop strongly around the Mott boundary. Because such a feature has never been detected in previous research on the Mott transition and we focus most of the Discussion on this anomaly, the latter component (the blue component in Fig. 3B) increases its prominence at low pressure, where the system is insulating. Because the charge degree of freedom is gapped out in the Mott-insulating phase, the latter component
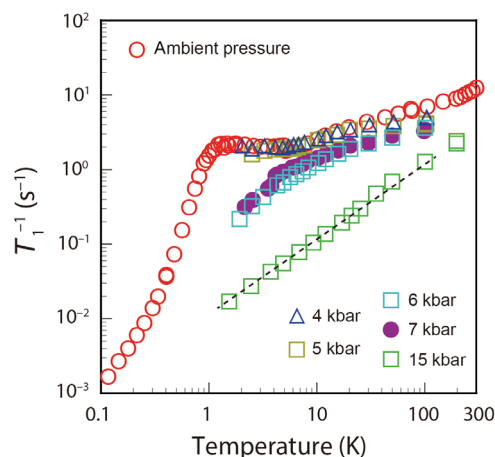
Fig. 1. Structure and transport properties of EtMe₃Sb[Pd(dmit)₂]₂. (A) Side view of the layered structure of EtMe$_3$Sb[Pd(dmit)$_2$]$_2$ (41). Mott-insulating Pd(dmit)$_2$ layers are separated by closed-shell cation layers of EtMe$_3$Sb. The cation layers have random orientations of the ethyl groups. (B) Temperature dependence of the in-plane resistivity of EtMe$_3$Sb[Pd(dmit)$_2$]$_2$ under several pressures measured using the standard four-electrode method.

Fig. 2. Temperature dependence of the ^{13}C nuclear spin-lattice relaxation rate (T_1^{-1}) of EtMe$_3$Sb[Pd(dmit)$_2$]$_2$ under several pressures, reflecting the amplitude of the fluctuations of the internal magnetic field on a megahertz time scale. The dashed line shows a fit of the data at 15 kbar to the Korringa relation $T_1^{-1} \propto T$.
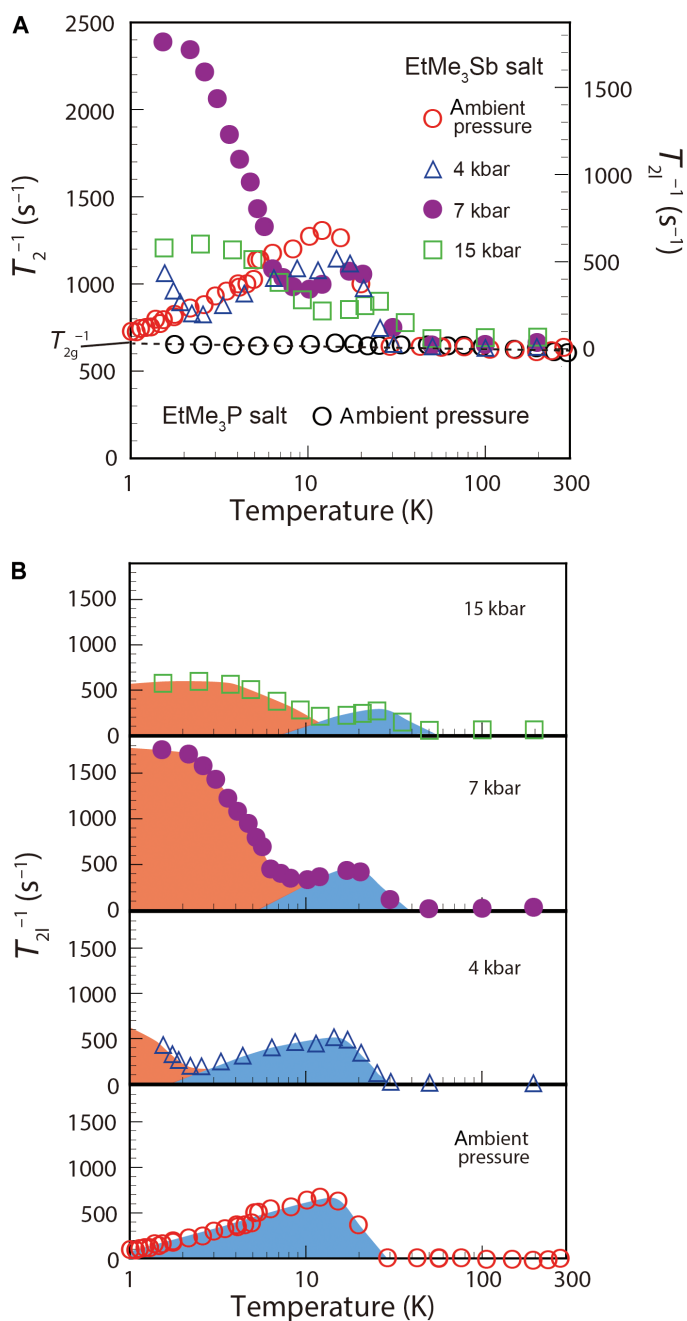
Fig. 3. Profiles of the ^{13}C nuclear spin-spin relaxation rate (T_2^{-1}) of EtMe$_3$Sb[Pd(dmit)$_2$]$_2$ under several pressures. (**A**) Temperature dependence of T_2^{-1} of EtMe$_3$Sb[Pd(dmit)$_2$]$_2$ under several pressures. For comparison, data for EtMe$_3$P[Pd(dmit)$_2$]$_2$ at ambient pressure are also plotted as open black circles. The left axis shows the observed raw value of the whole spin-spin relaxation rate. The value of T_{2l}^{-1} (the right axis) is estimated by subtracting 640 s^{-1} from T_2^{-1} (see Materials and Methods and the Supplementary Materials). (**B**) The two components of T_{2l}^{-1} of EtMe$_3$Sb[Pd(dmit)$_2$]$_2$. The amplitude of the blue component shows a peak at 10 to 30 K. The amplitude of the blue component at low temperatures (where both components exist) is estimated by extrapolating the trend at higher temperatures. The amplitude of the red component is enhanced at low temperatures. This enhancement is particularly prominent at 7 kbar, which is near the Mott boundary.

likely stems from spin fluctuations. The overall schematic pressure-temperature phase diagram is summarized in Fig. 4, where red and blue represent the magnitudes of the slow fluctuations in the charge and spin sectors, respectively. Note that a recent theoretical work (26) has suggested that spinon fluctuations present deep on the Mott-insulating side are strongly suppressed by scattering from charge fluctuations as soon as the Mott gap closes.

DISCUSSION

The anomalous slow charge fluctuations observed in the Mott boundary contradict the conventional picture that the Mott transition is of the first order at low temperatures. To explain this anomaly, we exploit the concept of the Griffiths phase, which was originally developed in the area of spin physics, and invoke the notion of the "electronic Griffiths phase" as follows. It has been well recognized that the Mott
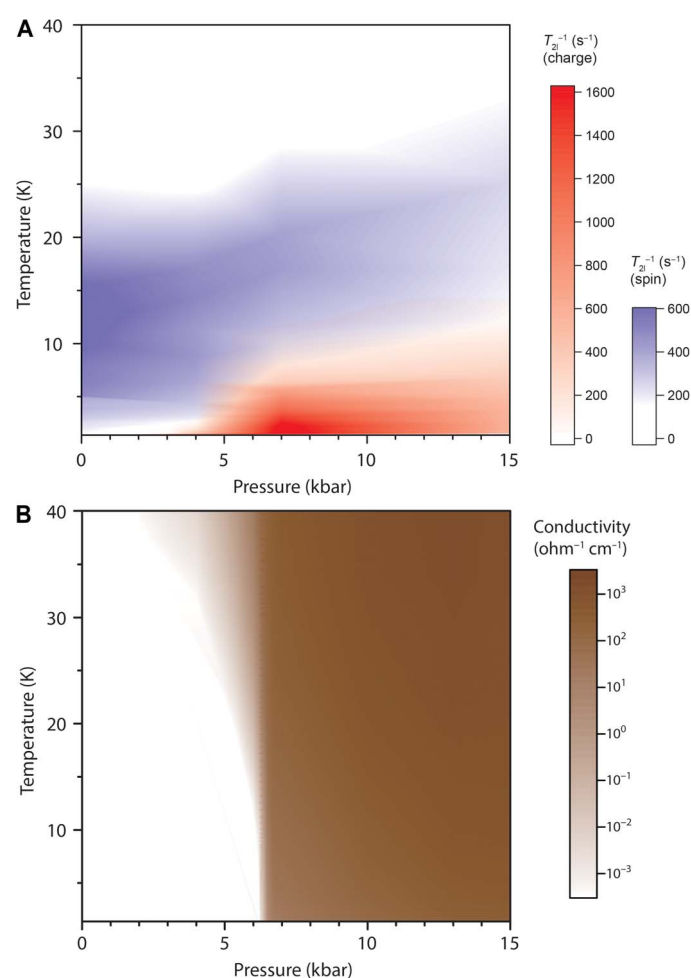

Fig. 4. Pressure-temperature phase diagram of the slow fluctuations in EtMe$_3$Sb[Pd(dmit)$_2$]$_2$. (**A**) Schematic pressure-temperature phase diagram of the contour plot of the slow fluctuations in EtMe$_3$Sb[Pd(dmit)$_2$]$_2$. The magnitudes of the charge and spin fluctuations are represented in red and blue, respectively. The intensities are determined by the amplitudes of the blue and red components of T_{2l}^{-1} in Fig. 3B. (**B**) Pressure-temperature phase diagram of the contour plot of the conductivity (the inverse of the resistivity shown in Fig. 1B), for comparison. Note that the horizontal axes in the two panels stand for the value of the pressure applied at room temperature, and the actual pressure in the temperature region discussed in these phase diagrams is 1.5 to 2 kbar lower than the value on the horizontal axes.

transition of repulsively interacting electrons is mapped onto the ferromagnetic transition of exchange-interacting Ising spins, and the pressure-temperature phase diagram of the Mott transition system corresponds to the field-temperature phase diagram of the Ising system (1, 12, 13, 27), as shown in Fig. 5 (A and B). This is because both the transitions have a scalar-nature order parameter, although the critical exponents of the Mott transition are controversial. When randomness is introduced into the Ising system, the randomness suppresses the first-order transition separating the ferromagnetic up-spin and down-spin states, pushing the critical end point of the first-order transition to absolute zero; in the case of strong randomness, the first-order transition completely vanishes. According to the celebrated concept introduced by Griffiths (28), the first-order transition line is replaced by a widely spread critical region—the Griffiths phase—in which spins are slowly fluctuating between the ferromagnetic up-spin and down-spin states (29), as shown in Fig. 5C.

We propose that this concept can be applied to the Mott transition because of the equivalence of the two systems, namely, introducing randomness replaces the original first-order Mott transition line with an electronic Griffiths phase, in which electrons slowly fluctuate between the metallic and Mott-insulating states, as shown in Fig. 5D. This picture assumes the first-order transition in the pristine system and is fully consistent with the DMFT, which predicts that the first-order Mott transition line ending at a finite temperature divides metallic and insulating phases (2). On the transition line, the two phases would coexist in a macroscopic scale in the pristine system; however, disorder would make the coexistence finely divided into microscopic

scales in the present system, possibly causing slow fluctuations between the insulating and metallic states. The DMFT also suggests the emergence of quantum critical metal-insulator fluctuations at high temperatures well above the critical end point (30, 31), which was later demonstrated by experiment (32). It is intriguing to know whether this quantum critical regime spreads to lower energies and, if so, how the Griffiths phase is affected by its quantum nature. On the other hand, a continuous Mott transition in a spin liquid is also theoretically proposed (33, 34). The above scenario based on the first-order transition is not straightforwardly applicable to the case of the continuous transition; however, we reserve the possibility that the slow dynamics can be a ubiquitous feature irrespective of the order of the metal-insulator transition in the pristine system. In actuality, a disordered 2D electron system in Si is reported to exhibit slow fluctuations in conductance (35–37).

The electronic Griffiths phase concept has also been proposed in a recent theoretical work (38), which predicts that the electronic Griffiths phase around the Mott boundary tends to spread toward the metallic side. Figure 4 shows that the present electronic Griffiths phase starts appearing at 4 kbar, attains prominence at 7 kbar, and then widely spreads toward the higher-pressure side. This behavior is consistent with the theoretical prediction. In addition, the theoretical work discusses the electronic Griffiths phase from the perspective of the "infinite randomness fixed point (IRFP)," around which the Griffiths singularities are much stronger than those in the usual Griffiths phase. The IRFP scenario is suggested to be generally realized in quantum phase transition systems with a lower critical dimension $d_c = 1$ (39).
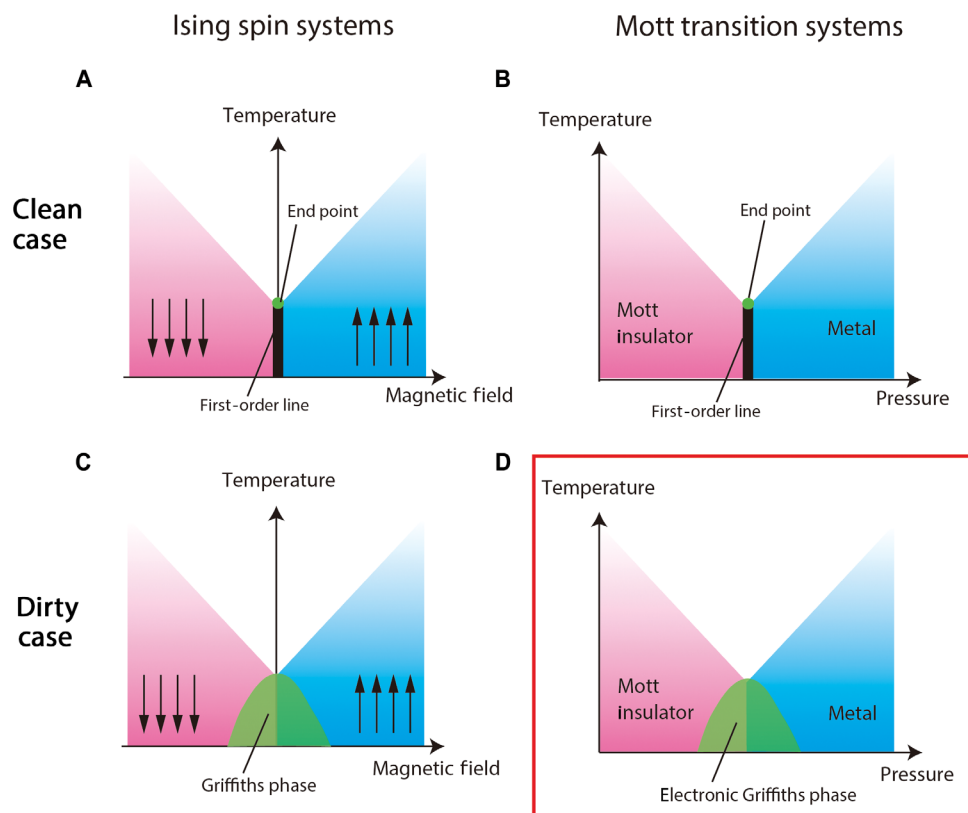

Fig. 5. Schematic phase diagrams of Ising spin systems and Mott transition systems. (**A**) Field-temperature phase diagram of a clean Ising spin system. (**B**) Pressure-temperature phase diagram of a clean Mott transition system. (**C**) Field-temperature phase diagram of an Ising spin system with randomness. (**D**) Our proposed pressure-temperature phase diagram of a Mott transition system with randomness.

For the Mott transition, $d_c = 1$, as is the case with the Ising transition. Although whether the present Mott transition would be a quantum phase transition in the clean limit is unclear, it is expected to have the quantum transition nature in that this material fulfils the quantum critical scaling of resistivity (32). Note again that a theoretical framework of the Mott instability from spin liquids assumes a continuous Mott transition (33, 34). Therefore, the IRFP scenario may be applicable to the present material and explain why the slow dynamics, which are one form of Griffiths singularity, are observed so strongly.

The peculiarity of the Mott transition in the present material may be related to the origin of the spin liquid ground state. Note that, in addition to the charge fluctuations, the present Mott insulator also yields slow spin fluctuations (the blue-colored region in Fig. 4). These are not observed in the $EtMe_3P$ salt, where the Mott transition is conventional and the ground state of the Mott-insulating phase is a clear spin-gapped state with valence bond–solid formation. The slow spin fluctuations observed in the $EtMe_3Sb$ salt are not conventional critical spin fluctuations toward the antiferromagnetic ordering because the fluctuations are weak and observed only for T_{2l}^{-1}. A slight amount of inhomogeneous spin freezing in the spin liquid background has been reported in organic spin liquid materials (19, 40). The slow spin fluctuations observed here likely capture the dynamic aspect of the inhomogeneous spin freezing and provide additional insight into the spin liquid nature in organics, which has been an unresolved problem.

MATERIALS AND METHODS
Sample preparation
We prepared fine high-quality single crystals of $EtMe_3Sb[Pd(dmit)_2]_2$ with typical sizes of 0.3 mm × 0.3 mm × 0.01 mm using an aerial oxidation method (41). For the ^{13}C NMR measurements, we enriched the inner carbon sites of the $Pd(dmit)_2$ molecule, which have large hyperfine coupling with electrons (23), as shown in Fig. 1A.

Resistivity measurements
A sample to which four electrical leads were attached was encased in a Teflon capsule filled with pressure medium. Resistivity measurements were carried out using a conventional dc method with the electrical current along the 2D plane.

Overall NMR measurements
We packed a number of fine single crystals into a Teflon tube with no particular orientation. The Teflon tube was encased in a Teflon capsule filled with pressure medium. The NMR measurements were performed at a field of 7.65 T (corresponding to the ^{13}C NMR frequency of 80.4 MHz). The NMR signals were obtained by the spin-echo method with a π/2-π pulse sequence. The typical pulse widths of the π/2 and π pulses were 2.5 and 5 μs, respectively. These values were sufficiently smaller than the inverse of the spectral widths, and thus, the pulses could cover the whole NMR spectra.

Applying pressure
The Teflon capsules for the resistivity and NMR measurements mentioned above were set in clamp-type pressure cells, and hydrostatic pressure was applied at room temperature. The pressure medium used was Idemitsu Daphne 7373 oil. Note that the applied pressures decrease by 1.5 to 2 kbar from the room temperature values around the oil solidification temperature (200 to 300 K) upon cooling. The pressure values shown in this paper are those at room temperature.

Spin-lattice relaxation rate
The spin-lattice relaxation rates (T_1^{-1}) were obtained from the recovery of the spin-echo intensity as a function of t, where t is the time interval between the saturation comb pulses and the π/2-π pulses to form echoes. The spin-lattice decay curves, defined by $1 - M(t)/M(\infty)$, are not single exponential functions because of the distribution of the angle between the sample direction and the applied magnetic field and the existence of four different crystallographical ^{13}C sites. Therefore, we define T_1^{-1} as the time when the recovery curves reach $1/e$.

Spin-spin relaxation rate
The spin-spin relaxation rates (T_2^{-1}) were obtained from the decay of the spin-echo intensity as a function of 2τ, where τ is the time interval between the π/2 and π pulses. We define T_2 as the time when the spin-spin decay curves [$M(2\tau)$] reach $1/e$, as for T_1 (for details, see the Supplementary Materials).

SUPPLEMENTARY MATERIALS
Supplementary material for this article is available at http://advances.sciencemag.org/cgi/content/full/3/8/e1601594/DC1
section S1. Spin-spin relaxation
section S2. Cation molecular motion
fig. S1. ^{13}C spin-spin relaxation curves as functions of 2τ (left) and $(2\tau)^2$ (right) for $EtMe_3Sb[Pd(dmit)_2]_2$ and $EtMe_3P[Pd(dmit)_2]_2$.
fig. S2. Temperature dependence of the spin-lattice relaxation rate (T_1^{-1}) of the protons in the cation molecule of $EtMe_3Sb[Pd(dmit)_2]_2$ at several pressures.
Reference (42)

REFERENCES AND NOTES
1. C. Castellani, C. Di Castro, D. Feinberg, J. Ranninger, New model Hamiltonian for the metal-insulator transition. Phys. Rev. Lett. 43, 1957–1960 (1979).
2. A. Georges, G. Kotliar, W. Krauth, M. J. Rozenberg, Dynamical mean-field theory of strongly correlated fermion systems and the limit of infinite dimensions. Rev. Mod. Phys. 68, 13–125 (1996).
3. M. Imada, A. Fujimori, Y. Tokura, Metal-insulator transitions. Rev. Mod. Phys. 70, 1039–1263 (1998).
4. S. Lefebvre, P. Wzietek, S. Brown, C. Bourbonnais, D. Jérome, C. Mézière, M. Fourmigué, P. Batail, Mott transition, antiferromagnetism, and unconventional superconductivity in layered organic superconductors. Phys. Rev. Lett. 85, 5420–5423 (2000).
5. F. Kagawa, T. Itou, K. Miyagawa, K. Kanoda, Transport criticality of the first-order Mott transition in the quasi-two-dimensional organic conductor κ-(BEDT-TTF)₂Cu[N(CN)₂]Cl. Phys. Rev. B 69, 064511 (2004).
6. K. Kanoda, R. Kato, Mott physics in organic conductors with triangular lattices. Annu. Rev. Condens. Matter Phys. 2, 167–188 (2011).
7. F. Kagawa, K. Miyagawa, K. Kanoda, Unconventional critical behaviour in a quasi-two-dimensional organic conductor. Nature 436, 534–537 (2005).
8. F. Kagawa, K. Miyagawa, K. Kanoda, Magnetic Mott criticality in a κ-type organic salt probed by NMR. Nat. Phys. 5, 880–884 (2009).
9. T. Misawa, M. Imada, Quantum criticality around metal-insulator transitions of strongly correlated electron systems. Phys. Rev. B 75, 115121 (2007).
10. M. Sentef, P. Werner, E. Gull, A. P. Kampf, Charge and spin criticality for the continuous Mott transition in a two-dimensional organic conductor. Phys. Rev. B 84, 165133 (2011).
11. L. Bartosch, M. de Souza, M. Lang, Scaling theory of the Mott transition and breakdown of the Grüneisen scaling near a finite-temperature critical end point. Phys. Rev. Lett. 104, 245701 (2010).
12. P. Limelette, A. Georges, D. Jérome, P. Wzietek, P. Metcalf, J. M. Honig, Universality and critical behavior at the Mott transition. Science 302, 89–92 (2003).
13. M. Abdel-Jawad, R. Kato, I. Watanabe, N. Tajima, Y. Ishii, Universality class of the Mott transition. Phys. Rev. Lett. 114, 106401 (2015).
14. S. Papanikolaou, R. M. Fernandes, E. Fradkin, P. W. Phillips, J. Schmalian, R. Sknepnek, Universality of liquid-gas Mott transitions at finite temperatures. Phys. Rev. Lett. 100, 026408 (2008).
15. M. Zacharias, L. Bartosch, M. Garst, Mott metal-insulator transition on compressible lattices. Phys. Rev. Lett. 109, 176401 (2012).
16. P. Sémon, A.-M. S. Tremblay, Importance of subleading corrections for the Mott critical point. Phys. Rev. B 85, 201101(R) (2012).

17. R. Kato, Development of π-electron systems based on [M(dmit)$_2$] (M = Ni and Pd; dmit: 1,3-dithiole-2-thione-4,5-dithiolate) anion radicals. *Bull. Chem. Soc. Jpn.* **87**, 355–374 (2014).

18. M. Tamura, A. Nakao, R. Kato, Frustration-induced valence-bond ordering in a new quantum triangular antiferromagnet based on [Pd(dmit)$_2$]. *J. Phys. Soc. Jpn.* **75**, 093701 (2006).

19. T. Itou, A. Oyamada, S. Maegawa, M. Tamura, R. Kato, Quantum spin liquid in the spin-1/2 triangular antiferromagnet EtMe$_3$Sb[Pd(dmit)$_2$]$_2$. *Phys. Rev. B* **77**, 104413 (2008).

20. M. Yamashita, N. Nakata, Y. Senshu, M. Nagata, H. M. Yamamoto, R. Kato, T. Shibauchi, Y. Matsuda, Highly mobile gapless excitations in a two-dimensional candidate quantum spin liquid. *Science* **328**, 1246–1248 (2010).

21. T. Itou, A. Oyamada, S. Maegawa, R. Kato, Instability of a quantum spin liquid in an organic triangular-lattice antiferromagnet. *Nat. Phys.* **6**, 673–676 (2010).

22. S. Yamashita, T. Yamamoto, Y. Nakazawa, M. Tamura, R. Kato, Gapless spin liquid of an organic triangular compound evidenced by thermodynamic measurements. *Nat. Commun.* **2**, 275 (2011).

23. T. Itou, K. Yamashita, M. Nishiyama, A. Oyamada, S. Maegawa, K. Kubo, R. Kato, Nuclear magnetic resonance of the inequivalent carbon atoms in the organic spin-liquid material EtMe$_3$Sb[Pd(dmit)$_2$]$_2$. *Phys. Rev. B* **84**, 094405 (2011).

24. D. Watanabe, M. Yamashita, S. Tonegawa, Y. Oshima, H. M. Yamamoto, R. Kato, I. Sheikin, K. Behnia, T. Terashima, S. Uji, T. Shibauchi, Y. Matsuda, Novel Pauli-paramagnetic quantum phase in a Mott insulator. *Nat. Commun.* **3**, 1090 (2012).

25. Y. Shimizu, H. Akimoto, H. Tsujii, A. Tajima, R. Kato, Mott transition in a valence-bond solid insulator with a triangular lattice. *Phys. Rev. Lett.* **99**, 256403 (2007).

26. T.-H. Lee, S. Florens, V. Dobrosavljević, Fate of spinons at the Mott point. *Phys. Rev. Lett.* **117**, 136601 (2016).

27. G. Kotliar, E. Lange, M. J. Rozenberg, Landau theory of the finite temperature Mott transition. *Phys. Rev. Lett.* **84**, 5180–5183 (2000).

28. R. B. Griffiths, Nonanalytic behavior above the critical point in a random Ising ferromagnet. *Phys. Rev. Lett.* **23**, 17–19 (1969).

29. M. Randeria, J. P. Sethna, R. G. Palmer, Low-frequency relaxation in Ising spin-glasses. *Phys. Rev. Lett.* **54**, 1321–1324 (1985).

30. H. Terletska, J. Vučičević, D. Tanasković, V. Dobrosavljević, Quantum critical transport near the Mott transition. *Phys. Rev. Lett.* **107**, 026401 (2011).

31. J. Vučičević, H. Terletska, D. Tanasković, V. Dobrosavljević, Finite-temperature crossover and the quantum Widom line near the Mott transition. *Phys. Rev. B* **88**, 075143 (2013).

32. T. Furukawa, K. Miyagawa, H. Taniguchi, R. Kato, K. Kanoda, Quantum criticality of Mott transition in organic materials. *Nat. Phys.* **11**, 221–224 (2015).

33. T. Senthil, Theory of a continuous Mott transition in two dimensions. *Phys. Rev. B* **78**, 045109 (2008).

34. R. V. Mishmash, I. González, R. G. Melko, O. I. Motrunich, M. P. A. Fisher, Continuous Mott transition between a metal and a quantum spin liquid. *Phys. Rev. B* **91**, 235140 (2015).

35. S. Bogdanovich, D. Popović, Onset of glassy dynamics in a two-dimensional electron system in silicon. *Phys. Rev. Lett.* **88**, 236401 (2002).

36. J. Jaroszyński, D. Popović, T. M. Klapwijk, Universal behavior of the resistance noise across the metal-insulator transition in silicon inversion layers. *Phys. Rev. Lett.* **89**, 276401 (2002).

37. P. V. Lin, X. Shi, J. Jaroszynski, D. Popović, Conductance noise in an out-of-equilibrium two-dimensional electron system. *Phys. Rev. B* **86**, 155135 (2012).

38. E. C. Andrade, E. Miranda, V. Dobrosavljević, Electronic Griffiths phase of the $d = 2$ Mott transition. *Phys. Rev. Lett.* **102**, 206403 (2009).

39. T. Vojta, Quantum Griffiths effects and smeared phase transitions in metals: Theory and experiment. *J. Low Temp. Phys.* **161**, 299–323 (2010).

40. Y. Shimizu, K. Miyagawa, K. Kanoda, M. Maesato, G. Saito, Emergence of inhomogeneous moments from spin liquid in the triangular-lattice Mott insulator κ-(ET)$_2$Cu$_2$(CN)$_3$. *Phys. Rev. B* **73**, 140407(R) (2006).

41. R. Kato, C. Hengbo, Cation dependence of crystal structure and band parameters in a series of molecular conductors, β'-(Cation)[Pd(dmit)$_2$]$_2$ (dmit = 1,3-dithiole-2-thione-4,5-dithiolate). *Crystals* **2**, 861–874 (2012).

42. M. Poirier, M.-O. Proulx, R. Kato, Ultrasonic investigation of the organic spin-liquid compound EtMe$_3$Sb[Pd(dmit)$_2$]$_2$. *Phys. Rev. B* **90**, 045147 (2014).

Citation: T. Itou, E. Watanabe, S. Maegawa, A. Tajima, N. Tajima, K. Kubo, R. Kato, K. Kanoda, Slow dynamics of electrons at a metal–Mott insulator boundary in an organic system with disorder. *Sci. Adv.* **3**, e1601594 (2017).